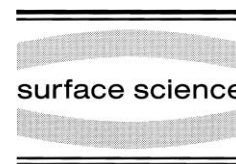




ELSEVIER

Surface Science 437 (1999) 18–28



www.elsevier.nl/locate/susc

# The reconstruction of nickel and rhodium (001) surfaces upon carbon, nitrogen or oxygen adsorptions

Dario Alfè<sup>1</sup>, Stefano de Gironcoli, Stefano Baroni\*

*SISSA — Scuola Internazionale Superiore di Studi Avanzati, and INFN — Istituto Nazionale di Fisica della Materia via Beirut 2–4, I-34014 Trieste, Italy*

Received 14 December 1998; accepted for publication 27 April 1999

## Abstract

Nickel and rhodium (001) surfaces display a similar (in terms of scanning tunneling microscopy images) *clock reconstruction* when half a monolayer of C–Ni, N–Ni or O–Rh is adsorbed; no reconstruction is observed instead for O–Ni. Adsorbate atoms sit at the center of the *black* squares of a chess-board,  $c(2 \times 2)$ , pattern and *two different* reconstructions are actually compatible with the observed STM images — showing a  $(2 \times 2)p4g$  pattern — according to whether a rotation of the *black* or *white* squares occurs. We report on a first-principles study of the structure of X–Ni(001) and X–Rh(001) surfaces (X=C, N, O) at half a monolayer coverage, performed using density-functional theory. Our findings are in agreement with all available experimental information and shed new light on the mechanisms responsible for the reconstructions. We show that the same substrate may display different reconstructions (or no reconstruction) upon adsorption of different atomic species, depending on the relative importance of the chemical and steric factors that determine the reconstruction. © 1999 Published by Elsevier Science B.V. All rights reserved.

**Keywords:** Carbon, nitrogen and oxygen adsorption; Clock reconstruction; Nickel; Rhodium; Surface reconstruction; Density functional calculations

## 1. Introduction

Transition metal surfaces are attracting a wide scientific and technical interest, especially because of their capability of reducing the activation barrier of many important chemical reactions. One particularly relevant example is the reaction  $2\text{CO} + 2\text{NO} \rightarrow 2\text{CO}_2 + \text{N}_2$ , which eliminates the two poisonous CO and NO gases from the exhaust gas

of combustion engines. This reaction is catalyzed by many transition metal surfaces, among which rhodium and platinum have been demonstrated to be the most efficient.

Adsorption of atomic or molecular species on surfaces modifies their electronic and structural properties, thus affecting their catalytic properties. Recently, the (001) surfaces of rhodium and nickel have been studied with respect to their peculiar reconstructions upon oxygen, carbon and nitrogen adsorption [1–10]. Oxygen adsorption on Rh (001) is known to be dissociative and to saturate at half a monolayer, independently of the adsorption temperature. At this coverage a  $(2 \times 2)$  reconstruction has been observed by low-energy electron

\* Corresponding author.

*E-mail addresses:* d.alf@ucl.ac.uk (D. Alfe), degironc@sissa.it (S. de Gironcoli), baroni@sissa.it (S. Baroni)

<sup>1</sup> Present address: Department of Geological Sciences, University College London, Gower Street, London WC1E 6BT, UK.

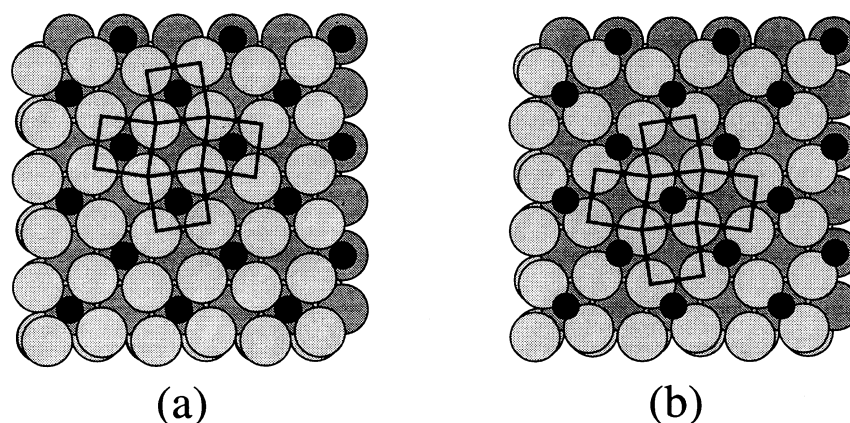


Fig. 1. Two possible *clock* reconstructions of the O–Rh(001) surface, resulting in a  $(2 \times 2)p4g$  structure. In the *black* reconstruction (a) the squares with an O atom in the middle rotate, whereas the empty ones distort to rhombi; in the *white* reconstruction (b), the opposite occurs.

diffraction (LEED) [2] and confirmed by scanning tunneling microscopy (STM) [3]. The oxygen atoms sit in the troughs formed by four first-layer rhodium atoms and fill these sites in a  $c(2 \times 2)$  geometry. This structure may be seen as a chess-board whose *black* squares are occupied by oxygen atoms, while the *white* ones are empty. Within this picture, the reconstruction observed in Ref. [3] has been described as a rotation of *black* squares, resulting in a  $(2 \times 2)p4g$  symmetry (see Fig. 1a). This distortion preserves the shape of the *black* squares, while the *white* ones become rhomboid. A similar behavior is observed for nitrogen and carbon adsorbed on the (001) surface of nickel, where the rotation angle of the squares is much larger and the *clock* reconstruction more evident [5–10].

In our previous work on Rh(001)–O [4] we pointed out that a different substrate reconstruction is actually compatible with LEED and STM data. Using only these two experimental techniques it is not possible to distinguish between the reconstruction described above and the one that results instead from the rotation of the *white* squares (Fig. 1b). Our calculations actually indicated that it is the *white* squares that rotate rather than the *black* ones. Moreover, we predicted a reconstruction pattern with a slightly different symmetry from what appears in the STM pictures. We found that the ad-atoms get off the center of the distorted squares, thus resulting in an *asymmetric clock*

reconstruction (Fig. 2). The oxygen atoms can occupy two equivalent low-symmetry sites separated by a low energy barrier, of the order of the room thermal energy. This would give rise to an order–disorder transition, and we suggested that what is actually observed in the STM pictures is the average position of the oxygen atoms jumping back and forth between the two equilibrium positions, in the high-temperature disordered phase.

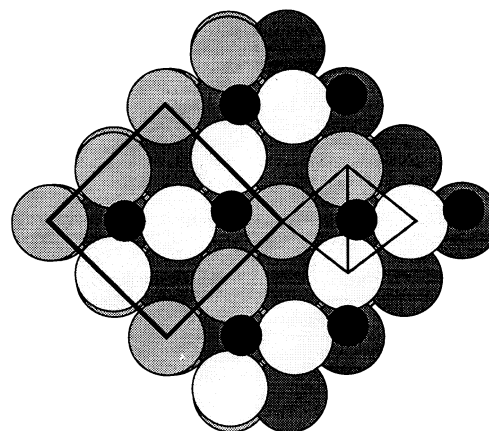


Fig. 2. Equilibrium structure of O–Rh(001) as obtained by our simulated-annealing procedure. The thick line indicates the unit cell. The thin line indicates the rhombus and its shorter diagonal. The oxygen atoms are alternatively shifted orthogonally with respect to the shorter diagonal. The atoms of the first surface layer depicted with a brighter tone lean  $\sim 0.08$  Å outwards with respect to the others.

The reconstruction of the (001) surface of nickel upon C and N adsorption is experimentally much better characterized since also LEED-*IV* [6] and SEXAFS [9] data exist. In this case it is widely accepted that the reconstruction is of the *black* type, i.e. it is the filled squares that rotate (Fig. 1a). No surface reconstruction is induced by oxygen adsorption on Ni(001) [11], whereas, as far as we know, no experimental data exist for carbon or nitrogen adsorbed on the Rh(001) surface.

In this paper we present an ab initio study of the adsorption of carbon, oxygen, and nitrogen on the (001) surfaces of rhodium and nickel. On rhodium, we find that *neither* nitrogen *nor* carbon induce any reconstruction of the surface. On nickel, in agreement with the experiments, we find that *both* carbon and nitrogen induce a *clock* reconstruction, whereas oxygen adsorbs with no induced reconstruction. We discuss the interplay of the chemical and the steric effects, which is at the root of these behaviors.

The paper is organized as follows. In Section 2 we describe our theoretical method, including some tests on the properties of the rhodium and nickel bulk metals, and on those of the CO, O<sub>2</sub>, NO and N<sub>2</sub> molecules. In Section 3 we present our results; Section 4 contains the discussion and our conclusions.

## 2. Method

Our calculations are based on density functional theory within the local-density approximation (LDA) [12,13], using Ceperley–Alder exchange–correlation (XC) energies [14]. The one-particle Kohn–Sham equations are solved self-consistently using plane-wave basis sets in an ultrasoft (US) pseudo-potential scheme [15]. The rhodium, oxygen, and carbon pseudo-potentials are the same as in Refs. [16,17]. For nitrogen and nickel we have constructed new pseudo-potentials. In the case of Ni, we started from the 3d<sup>8</sup>4s<sup>2</sup>4p<sup>0</sup> reference configuration, treating the d channel in the US scheme, whereas the s and the p channels were assumed to be norm conserving. We chose the p component of the pseudo-potential as the local part (this choice avoids the appearance of *ghost* states). For N we started from the 2s<sup>2</sup>2p<sup>3</sup> reference configuration treating both the s and the p channels in the US

scheme. Plane waves up to maximum kinetic energy of 30 Ry are included in the basis set. Brillouin-zone integrations have been performed using the Gaussian-smearing [18] special-point [19] technique. For the calculations in the bulk, we have used a smearing function of order 1 with a width  $\sigma=0.03$  Ry and a set of special points equivalent to ten  $k$ -points in the irreducible wedge of the Brillouin zone (IBZ). The convergence of our results with respect to the size of the basis and special-point sets has been carefully checked.

The isolated surfaces are modelled by a periodically repeated super-cell. We have used the same super-cell for both the clean and the covered surfaces. For the clean surfaces we have used five atomic layers plus a vacuum region corresponding to six layers. For the covered surfaces, the five Rh–Ni layers are completed by one layer of C, O, or N atoms on each side of the slab; in this case the vacuum region is correspondingly reduced to approximately five atomic layers. We have used a Gaussian-smearing function of width  $\sigma=0.03$  Ry and a (12, 12, 2) Monkhorst–Pack mesh [19] resulting in 21 special  $k$ -points in the 1 × 1 surface IBZ. Convergence tests performed with a value of  $\sigma$  half this size and a correspondingly finer mesh of special points resulted in no significant changes in total energies and equilibrium geometries.

### 2.1. Case tests on bulk metals and molecules

In order to test the quality of our pseudo-potentials, we have done some tests on rhodium and nickel bulks, as well as on CO, NO, O<sub>2</sub> and N<sub>2</sub> molecules. To calculate the properties of the molecules the latter have been put in a large cubic cell, with side  $L=10$  a.u., and periodic boundary conditions. We have checked that our calculated molecular properties were well converged with respect to the size of the cell. The results of these tests are summarized in Tables 1 and 2. Nickel and rhodium have the fcc crystal structure. To calculate the equilibrium lattice constant  $a_0$  and the bulk modulus  $B_0$ , we have fitted the calculated energies as a function of the unit cell volume to Murnaghan’s equation of state. Nickel is a magnetic metal with a magnetic moment of 0.59  $\mu_B$ /atom [22]. An explicit account of the spin polarization within the local spin density approxi-

Table 1

Theoretical structural parameters of fcc rhodium and nickel obtained with a fit to the Murnaghan equation of state of the calculated energies as a function of the volume. Experimental data [20] are reported for comparison

		Lattice constant (Å)	Bulk modulus (Mbar)
Rh	Present work	3.81	3.17
	Experiment	3.80	2.69
Ni	Present work	3.44	2.4
	Experiment	3.52	1.88

Table 2

Theoretical equilibrium distances and fundamental vibrational frequencies. Experimental data [21] are reported for comparison

		Equilibrium distance (Å)	Vibrational frequency (cm <sup>-1</sup> )
CO	Present work	1.14	2200
	Experiment	1.13	2170
NO	Present work	1.16	2000
	Experiment	1.15	1904
O <sub>2</sub>	Present work	1.23	1650
	Experiment	1.21	1580
N <sub>2</sub>	Present work	1.11	2450
	Experiment	1.09	2360

mation did not result in any meaningful changes of the calculated structural properties. The magnetism is expected to be more important at the surface, because the surface density of states (SDOS) is narrower than the bulk one. However, at least for the carbon- and the nitrogen-covered surfaces, we have found that the Ni-d-SDOS is shifted towards lower energies with respect to the bulk d partial density of states (see Fig. 3) thus resulting in a lower density of states at the Fermi level. We argue that magnetic effects should not be very important and they have been neglected altogether in the present investigation.<sup>2</sup>

<sup>2</sup> Explicit tests performed after this work was completed confirmed this guess. In the case of C–Ni, the inclusion of magnetic effects at the LSDA level did not result in any significant modifications of the predicted structure. For N–Ni, magnetic effects are larger, possibly due to the high spin of nitrogen atoms. As a consequence, the structural parameters predicted by LSDA calculations slightly differ from those predicted by the LDA: the  $\delta$  and  $d_{01}$  parameters reported in Table 3 would change from 0.41 and 0.10 to 0.33 and 0.31 respectively. In any case, the overall reconstruction pattern and the relative stability of different structures do not change when magnetic effects are explicitly considered.

### 3. Results

In order to find the stable surface structure of the C-, O-, and N-covered Rh(001) and Ni(001) surfaces, we have performed simulated annealing runs of the surfaces at half a monolayer of coverage, using Born–Oppenheimer ab initio molecular

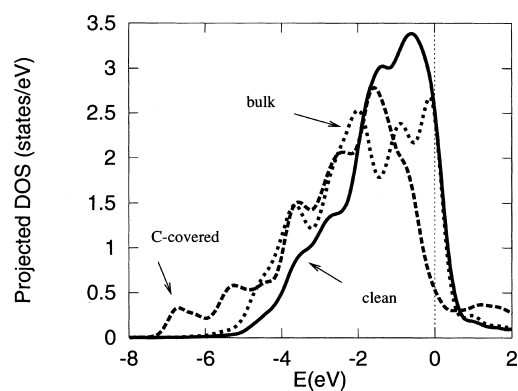


Fig. 3. The d-projected density of states of nickel for the bulk, the clean surface, and the carbon-covered surface.

Table 3

Summary of the structural data for the six systems investigated in this work. For the reconstruction type see Fig. 1.  $d_{01}$  is the distance between the ad-atoms and the first metal layer;  $\delta$  is the amplitude of the in-plane displacement of the first-layer metal atoms upon reconstruction;  $\Delta E$  is the energy difference between the symmetric  $c(2 \times 2)$  structure and the reconstructed one

	Reconstruction		$\delta$ (Å)		$d_{01}$ (Å)		$\Delta E$
	Expt	Theory	Expt	Theory	Expt	Theory	(eV/atom) Theory
C–Ni	<i>black</i>	<i>black</i>	$0.55 \pm 0.20^a$	0.46	$0.1 \pm 0.1^a$	0.17	0.20
N–Ni	<i>black</i>	<i>black</i>	$0.55 \pm 0.20^a$	0.41	$0.1 \pm 0.1^a$	0.10	0.08
O–Ni	none	none			$0.77 \pm 0.04^b$	0.73	
C–Rh		none				0.63	
N–Rh		none				0.71	
O–Rh	<i>white</i> <sup>c</sup>	<i>white</i>	$0.20 \pm 0.07^{c,d}$	0.21	$1.05 \pm 0.05^e$ $0.6 \pm 0.1^d$	$0.98-1.06^e$	0.03

<sup>a</sup> From Ref. [10] and references cited therein.

<sup>b</sup> From Ref. [11].

<sup>c</sup> From Ref. [27].

<sup>d</sup> See Ref. [28].

<sup>e</sup> The two values correspond to the two Rh rows made inequivalent by the *asymmetric* clock reconstruction (see text and Fig. 2).

dynamics (AIMD). In our implementation of AIMD the exact electronic ground state (within a self-consistent threshold) is calculated at each time step using a band-by-band conjugate gradient algorithm [23,24] and Broyden-like [25] mixing of the potentials. The forces are calculated fully quantum mechanically, and the ionic equation of motion is integrated using the Verlet algorithm [26]. We have used a time step of 50 a.u. ( $\sim 1.2$  fs). After an equilibration period of about 0.5 ps at a temperature of  $\sim 800$  K we have slowly cooled down the systems. Finally, when the ionic minimum structure is reached, an accurate structure optimization is performed, by allowing all the atoms in the slab to relax until the force acting on each of them is smaller than  $0.5 \times 10^{-3}$  Ry/ $a_0$ . Our results are summarized in Table 3 and discussed in detail in the following sections.

### 3.1. Rhodium

Results for the O–Rh(001) surface have been reported and extensively discussed in our previous work [4]. Oxygen atoms tend to shorten the bonds with the neighboring rhodium atoms; this results in deformation of the oxygen adsorption site, which becomes a rhombus. This deformation cor-

responds to a *clock* reconstruction of the *white* type (see Fig. 1). Actually, in order to further shorten the O–Rh bonds, ad-atoms get off the centers of the rhombi and occupy one of the two symmetry-equivalent threefold sites within a rhombus (see Fig. 2). We believe that this symmetry breaking is associated to an order–disorder transition whose critical temperature is presumably rather low and whose characterization, in any case, lies beyond the scope of the present study. In this paper, we limit ourselves to study one ordered structure, where oxygen atoms occupy the same threefold site in all the rhombi.<sup>3</sup> The asymmetric position of the oxygen ad-atoms results in a buckling reconstruction of the first surface layer whose rows are alternatively shifted up and down by  $\sim \pm 0.04$  Å, according to whether their atoms are two- or one-fold co-ordinated with oxygen atoms. This buckling is expected to disappear in the symmetric high-temperature structure. The re-bonding of oxygen atoms with the first-layer metal atoms, responsible for the observed *clock*

<sup>3</sup> Actually, there are four symmetry-equivalent high-symmetry structures, because there are two rhombi, and hence four equivalent threefold sites per surface unit cell.

reconstruction, can be better understood by inspection of the local density of states (LDOS).

The LDOS is the projection of the density of states onto localized atomic orbitals. In Fig. 4a we display the Rh( $4d_{xz}$ ) LDOS of one rhodium surface atom resulting from a calculation with the clean surface; this is degenerate with the Rh( $4d_{yz}$ ) orbital because of symmetry. The energy is referred to the Fermi level. In Fig. 4b we display the same two orbitals after half a monolayer of oxygen is deposited, without allowing the substrate to reconstruct. The Rh( $4d_{xz}$ ) orbital points towards the square site left empty, and its LDOS is very similar to what it would be for the clean surface. The Rh( $4d_{yz}$ ) orbital is directed towards the oxygen adsorption site, and the shape of its LDOS changes completely upon adsorption: the most important feature is the presence of two peaks, one at  $\sim -6$  eV and the second above the Fermi energy, at  $\sim 1$  eV. In Fig. 4c we display the LDOS projected onto O( $2p_x$ ) orbitals, which are degenerate with the O( $2p_y$ ) orbitals because of the symmetry of the oxygen site. This LDOS is characterized by a bonding and an anti-bonding peak, at energies of  $\sim -6$  eV and  $\sim +1$  eV respectively, which are in the same positions of the peaks observed in the Rh( $4d_{yz}$ ) LDOS. We interpret this fact as the evidence of the presence of a strong covalent bond between the oxygen atoms and the rhodium surface atoms. The different weight between the bonding and the anti-bonding peaks also indicates that there is a charge transfer from the substrate to the oxygen, so that the bond is partially ionic.

This fact is also supported by work function calculations, which show an increase of  $\sim 0.6$  eV when the surface is covered by oxygen. This implies that an excess of negative charge is present on the surface. In Fig. 4d we display the LDOS projected onto the O( $2p_x$ ) and O( $2p_y$ ) orbitals for the reconstructed surface. The reconstruction lifts the  $xy$  symmetry, and the O( $2p_x$ ) orbital — which corresponds to the shorter O–Rh bond — becomes more occupied than the O( $2p_y$ ) orbital. We conclude that the mechanism of the reconstruction is due to the re-bonding of the oxygen with the surface atoms, which tends to shorten the O–Rh

bond. This shortening could also be realized by a penetration of the oxygen deeper into the site, but this does not happen. The reason, maybe, is the excess of negative charge on the oxygen atoms, which prevents their penetration into the electronic sea of the metallic surface.

While the present work was being completed, we learned that our theoretical predictions have been recently confirmed by LEED  $I$ – $V$  experiments [27]. In particular, the analysis of the LEED  $I$ – $V$  spectra indicated that the reconstruction of the Rh surface upon oxygen adsorption is indeed of the *white* type. Furthermore, the stable adsorption site of the oxygen ad-atoms was found to be asymmetric with respect to the center of the rhombus, with a displacement  $\delta_o = 0.29 \pm 0.15$  Å, to be compared with our theoretical prediction,  $\delta_o = 0.35$  Å. These data are in partial agreement with the recently published results of an experiment based on a combination of LEED with low-energy alkali ion scattering and recoil spectroscopy [28]. In Ref. [28] no evidence was found of the *asymmetric white* clock reconstruction predicted by us and confirmed in Ref. [27]. Furthermore, the height of the O adsorption site off the metal surface was found to be smaller than our predictions, which, however, are again in agreement with the findings of Ref. [27].

At variance with oxygen, nitrogen does not induce any reconstruction upon adsorption on Rh(001). The equilibrium distance of the ad-atom from the metal surface is rather large, as is the case for oxygen (see Table 3). For carbon we have found a metastable state with a surface reconstruction of the *black* type (Fig. 1a) and a rather small distance between the ad-atoms and the metal surfaces (see the discussion of the *black* reconstructions typical of Ni in Section 3.2). However, the energy of this local minimum is higher than that of the unreconstructed surface, which corresponds to a larger ad-atom–surface equilibrium distance. The presence of this second stable deep site, even though the energy is higher, suggests that the choice of the actual adsorption site is a trade-off between the chemical energy gained due to the larger number of ad-atom–Rh bonds in the deep site, and the elastic energy lost due the distortion

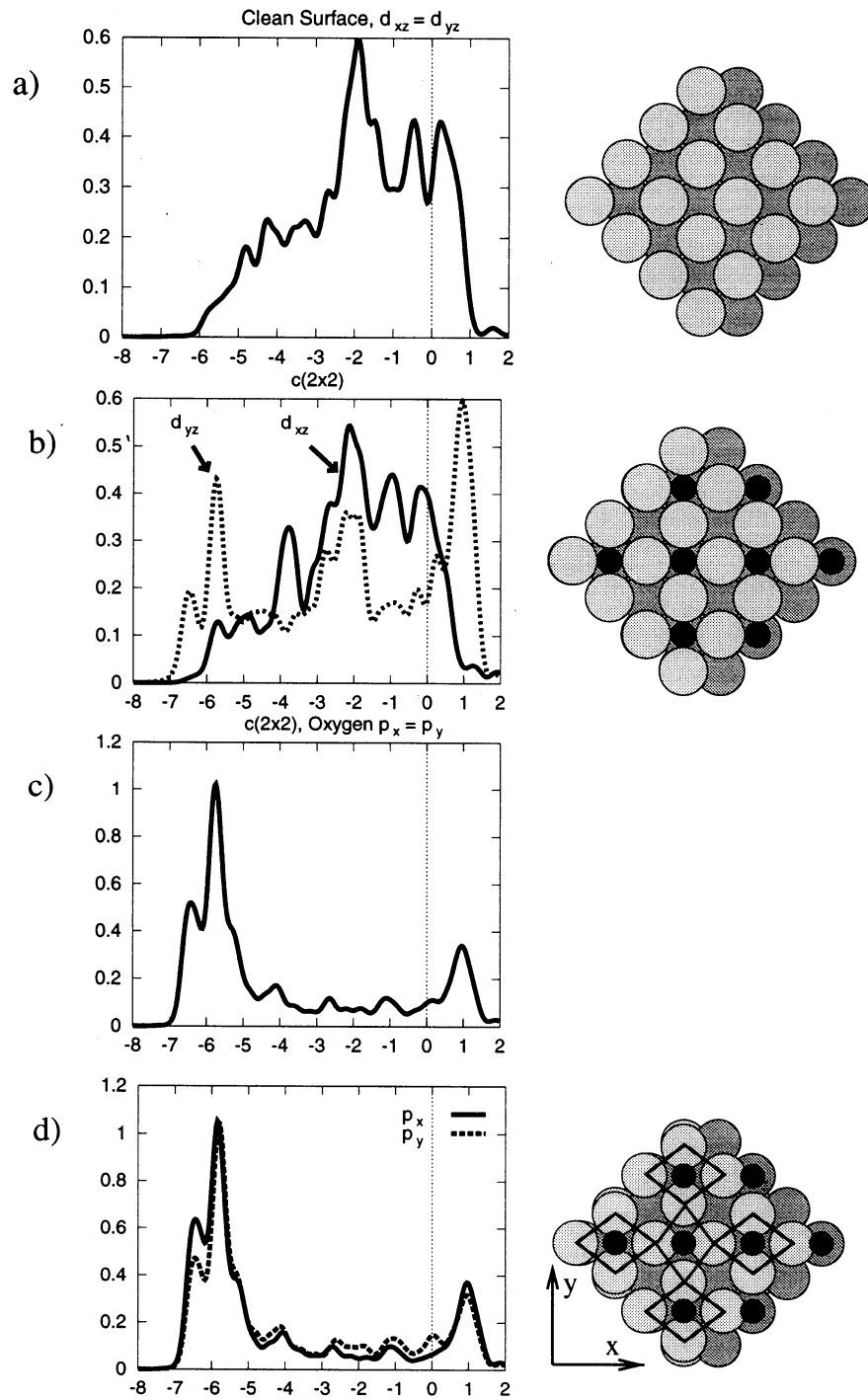


Fig. 4. LDOS projected onto surface atomic orbitals: (a) Rh  $d_{xz}$  and  $d_{yz}$  orbitals of the clean surface; (b) same as (a), but after the deposition of half a monolayer of oxygen, without allowing the substrate to reconstruct; (c) oxygen  $p_x$  and  $p_y$  orbitals; (d) same as (c), but after the clock reconstruction has taken place.

of the surface when this site is occupied. We shall comment more on this issue in Section 3.2.

### 3.2. Nickel

In agreement with experimental data [11], for O–Ni(001) we did not find any reconstruction at all. In this case the only effect that has been observed is a buckling in the second metal layer, whose atoms are not all coplanar but shifted up or down according to whether the fourfold site lying above is empty or filled [11,29–32]. This behavior is consistent with our interpretation of the O–Rh(001) reconstruction: the nickel lattice parameter is quite smaller than that of rhodium and, therefore, the adsorption site is already small enough for the oxygen ad-atoms to bind with neighboring metal atoms without inducing any reconstruction. For the carbon- and nitrogen-covered surfaces we have found a reconstruction where, contrary to O–Rh(001) and in agreement with experimental findings [6,9], it is the *filled* squares that rotate, i.e. a *black* reconstruction (Fig. 1a). In the case of carbon, we find that no energy barrier exists between the unreconstructed and the reconstructed structures, whereas such a barrier has been detected for N–Ni(001) — though its value has not been determined.

Going back to the results summarized in Table 3, an inspection of the results for  $d_{01}$  (the distance between the adsorbate atoms and the first metal layer) is particularly instructive. In those cases where a *black* reconstruction occurs (C–Ni and N–Ni),  $d_{01}$  is small ( $\sim 0.1$  Å), thus indicating that the adsorbates penetrate the first metal layer. The penetration of the adsorbate into the metal determines an *outward* (with respect to the center of the square) force acting on the metal atoms at the corners of the *black* squares. This can be alternatively described as an *inward* force as seen from the center of the *white* squares. In the case of a *white* reconstruction (O–Rh), instead, the ad-atoms stay out of the surface ( $d_{01} \approx 1$  Å), and they pull directly the neighboring atoms towards the adsorption site (rather than pushing them away from it) in order to strengthen the oxygen–metal bonds. In both cases, the square that is ‘squeezed’

by the adsorption process (*black* or *white*, depending on the case) displays an instability towards a rhomboid distortion that is partially opposed by the elastic reaction of the substrate.

It is worth noting that in the case where a *black* reconstruction occurs — and, hence,  $d_{01}$  is small — the unreconstructed structure is a metastable (N–Ni) or unstable (C–Ni) equilibrium structure characterized by a rather larger value of  $d_{01}$  (equal to 0.48 Å for both N–Ni and C–Ni). In order to understand the chemistry of the bond between carbon and nickel we have analyzed the LDOS for the unreconstructed and reconstructed surfaces, which we display in Fig. 5. In the two upper panels we show the LDOS projected onto the C  $p_x$  or  $p_y$  orbitals which are degenerate by symmetry (left) and onto the C  $p_z$  orbital (right). In both cases a bonding and an anti-bonding structure can be clearly identified. In the case of the C  $p_{x,y}$  orbitals, the bonding structure is resonant with similar structures observed in the LDOS projected onto the Ni  $d_{xy}$  and  $d_{x^2-y^2}$  orbitals, where the C  $p_z$  bonding structure is resonant with Ni  $d_{xz}$  (middle panels). Inspection of the difference between the C  $p_{x,y}$ - and C  $p_z$ -projected LDOS before and after reconstruction shows that the gain in binding energy upon reconstruction mainly comes from a shift of the C  $p_z$  LDOS towards lower energies, thus indicating the establishment of a covalent-like bond between the C  $p_z$  and Ni  $d_{xz}$  orbitals.

## 4. Discussion and conclusion

The behavior of the two surfaces studied here [Ni(001) and Rh(001)] is apparently very similar — they have the same STM images and LEED patterns — but a more accurate inspection of their structural and electronic properties reveals many interesting differences.

Firstly, in spite of the fact that the adsorption site of the ad-atoms is the same, the kind of reconstruction induced by them is different for O–Rh(001) and for C–Ni(001) or N–Ni(001). In the first case the oxygen site is deformed into a rhombus (*white* reconstruction), whereas in the second case the adsorption sites remain square, and it is

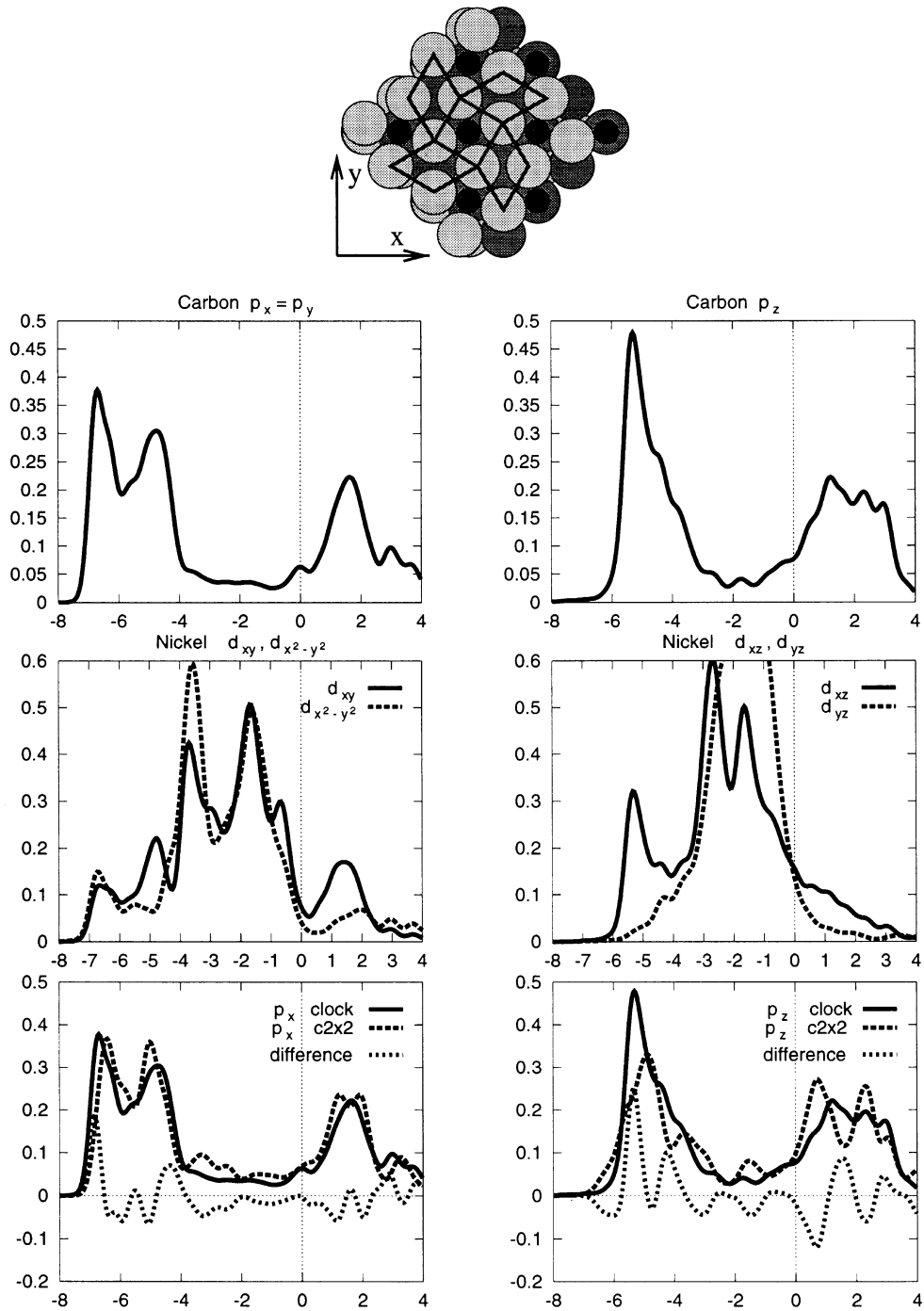


Fig. 5. Upper panels: LDOS of the C/Ni(001) surface, projected onto C  $p_x$  or  $p_y$  (left) and C  $p_z$  (right) atomic orbitals. Middle panels: same as above, but projected upon Ni  $d_{xy}$  and  $d_{x^2-y^2}$  orbitals (left) and Ni  $d_{xz}$  and  $d_{yz}$  orbitals (right). Lower panels: difference between the LDOS projected upon C  $p$  orbitals before and after the clock reconstruction takes place.

the empty sites that are deformed into rhombi (*black* reconstruction, see Fig. 1a).

Secondly, on rhodium the distance of the oxygen atoms from the surface is not appreciably different for the unreconstructed and the reconstructed surfaces, whereas on nickel we have found that when the reconstruction takes place carbon and nitrogen atoms become almost coplanar with those of the substrate, thus becoming essentially fivefold co-ordinated. The carbon atoms penetrate into the nickel substrate even at zero temperature, and they arrange themselves so as to be almost coplanar with the first nickel layer; the nitrogen atoms behave similarly, but a barrier is found to exist that gives rise to a metastable equilibrium structure in which the ad-atoms do not penetrate and the surface does not reconstruct. These facts indicate that the mechanism of the reconstruction is related to the atomic penetration into the first surface layer: the sites, which accommodate the ad-atoms, tend to enlarge, and this results necessarily in a rhomboid distortion of the empty sites. This distortion has a cost in terms of elastic effects. Upon C or N adsorption, the Ni(001) surface reconstructs, whereas Rh(001) does not. The reason is probably the different stiffnesses of the two metals: rhodium has larger elastic constants and thus it does not reconstruct. In the case of the oxygen the mechanism of the reconstruction is completely different, being due to the O–Rh re-bonding, and results in a different reconstruction pattern.

Further details on this work can be found in the Ph.D. thesis of one of us (DA) [33].

### Acknowledgements

We are grateful to Renzo Rosei for inspiring this work and for making the results of Ref. [27] available to us prior to publication. Many useful discussions with A. Baraldi, G. Comelli, and R. Rosei are gratefully acknowledged. Our calculations were performed on the SISSA IBM-SP2 and CINECA-INFM Cray-T3D/E parallel machines, in Trieste and Bologna respectively, using the parallel version of the PWSCF code. Access to

the Cray machines has been granted within the ‘Iniziativa Traversale Calcolo Parallelo’ of the INFM. Finally, we acknowledge support from the MURST within the initiative ‘Progetti di ricerca di rilevante interesse nazionale’.

### References

- [1] P.R. Watson, F.R. Shepherd, D.C. Frost, K.A.R. Mitchell, Surf. Sci. 72 (1978) 562.
- [2] W. Oed, B. Dötsch, L. Hammer, K. Heinz, K. Müller, Surf. Sci. 207 (1988) 55.
- [3] J.R. Mercer, P. Finetti, F.M. Leibsle, R. McGrath, V.R. Dhanak, A. Baraldi, K.C. Prince, R. Rosei, Surf. Sci. 352–354 (1996) 173.
- [4] D. Alfè, S. de Gironcoli, S. Baroni, Surf. Sci. 410 (1998) 151.
- [5] W. Daum, S. Lehwald, H. Ibach, Surf. Sci. 178 (1986) 528.
- [6] J.H. Onuferko, D.P. Woodruff, B.W. Holland, Surf. Sci. 87 (1979) 357.
- [7] C. Klink, L. Oleson, F. Besenbacher, I. Stensgaard, E. Laegsgaard, N.D. Lang, Phys. Rev. Lett. 71 (1993) 4350.
- [8] F.M. Leibsle, Surf. Sci. 297 (1993) 98.
- [9] L. Wenzel, D. Arvanitis, W. Daum, H.H. Rotermund, J. Stohr, K. Baberschke, H. Ibach, Phys. Rev. B 36 (1987) 7689.
- [10] A.L.D. Kilcoyne, D.P. Woodruff, A.W. Robinson, Th. Lindner, J.S. Somers, A.M. Bradshaw, Surf. Sci. 253 (1991) 107.
- [11] W. Oed, H. Lindner, U. Starke, K. Heinz, K. Müller, J.B. Pendry, Surf. Sci. 224 (1989) 253.
- [12] P. Hohenberg, W. Kohn, Phys. Rev. 136 (1964) B864.
- [13] W. Kohn, L. Sham, Phys. Rev. 140 (1965) A1133.
- [14] D. Ceperley, B. Alder, Phys. Rev. Lett. 45 (1980) 566.
- [15] D. Vanderbilt, Phys. Rev. B 41 (1990) 7892.
- [16] K. Stokbro, S. Baroni, Surf. Sci. 370 (1997) 166.
- [17] D. Alfè, S. Baroni, Surf. Sci. 382 (1997) L666.
- [18] M. Methfessel, A. Paxton, Phys. Rev. B 40 (1989) 3616.
- [19] H.J. Monkhorst, J.D. Pack, Phys. Rev. B 13 (1976) 5188.
- [20] <http://www.webelements.com>
- [21] B.H. Bransden, C.J. Joachain, Physics of Atoms and Molecules, Longman, New York, 1983, p. 393.
- [22] T. Sasaki, A.M. Rappe, S.G. Louie, Phys. Rev. B 52 (1995) 12 760.
- [23] M.P. Teter, M.C. Payne, D.C. Allan, Phys. Rev. B 40 (1989) 12 255.
- [24] M.J. Gillan, J. Phys. Condens. Matter 1 (1989) 689.
- [25] D.D. Johnson, Phys. Rev. B 38 (1988) 12 807.
- [26] L. Verlet, Phys. Rev. 159 (1967) 98.
- [27] A. Baraldi, J. Cerdá, J.A. Martín Gago, G. Comelli, S. Lizzit, G. Paolucci, R. Rosei, Phys. Rev. Lett. 82 (1999) 4874.
- [28] Y.G. Shen, A. Qayyum, D.J. O’Connor, B.V. King, Phys. Rev. B 58 (1998) 10 025.

- [29] K. Heinz, W. Oed, J.B. Pendry, Phys. Rev. B 41 (1990) 10179.
- [30] W. Oed, H. Lindner, U. Starke, K. Heinz, K. Müller, D.K. Saldin, P. de Andres, J.B. Pendry, Surf. Sci. 225 (1990) 242.
- [31] W. Oed, U. Starke, K. Heinz, K. Müller, J. Phys. Condens. Matter 3 (1991) s223.
- [32] E. Kopatzki, R.J. Behm, Surf. Sci. 245 (1991) 255.
- [33] D. Alfè, Ph.D. Thesis, SISSA, Trieste, 1997. Available on the internet at: <http://www.sissa.it/cm/PHD.html>.